

# Design and Control of the Lift Subsystem of a Two-Wheeled Forklift Robot

Sergio Esteban Quintero Benavides

## Content

- I. Introduction
- II. Lift mechanical design
- III. Modeling
- IV. Control
- V. Simulation results
- VI. Conclusions and Future Work

Supervisor: Professor Toshiyuki Murakami

Co-supervisor: Professor Teresa Zielińska

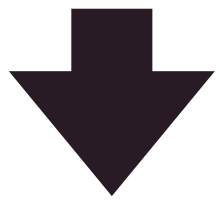
Keio University  
Graduate School of Science and  
Technology  
School of Integrated Design Engineering





# I. Introduction

In modern industrial environments, humans and robots work together.



- Labor shortage in industrialized countries.
- High-risk tasks executed by robots.



[A]

Mobile robots should have a small footprint for safety and space optimization reasons.



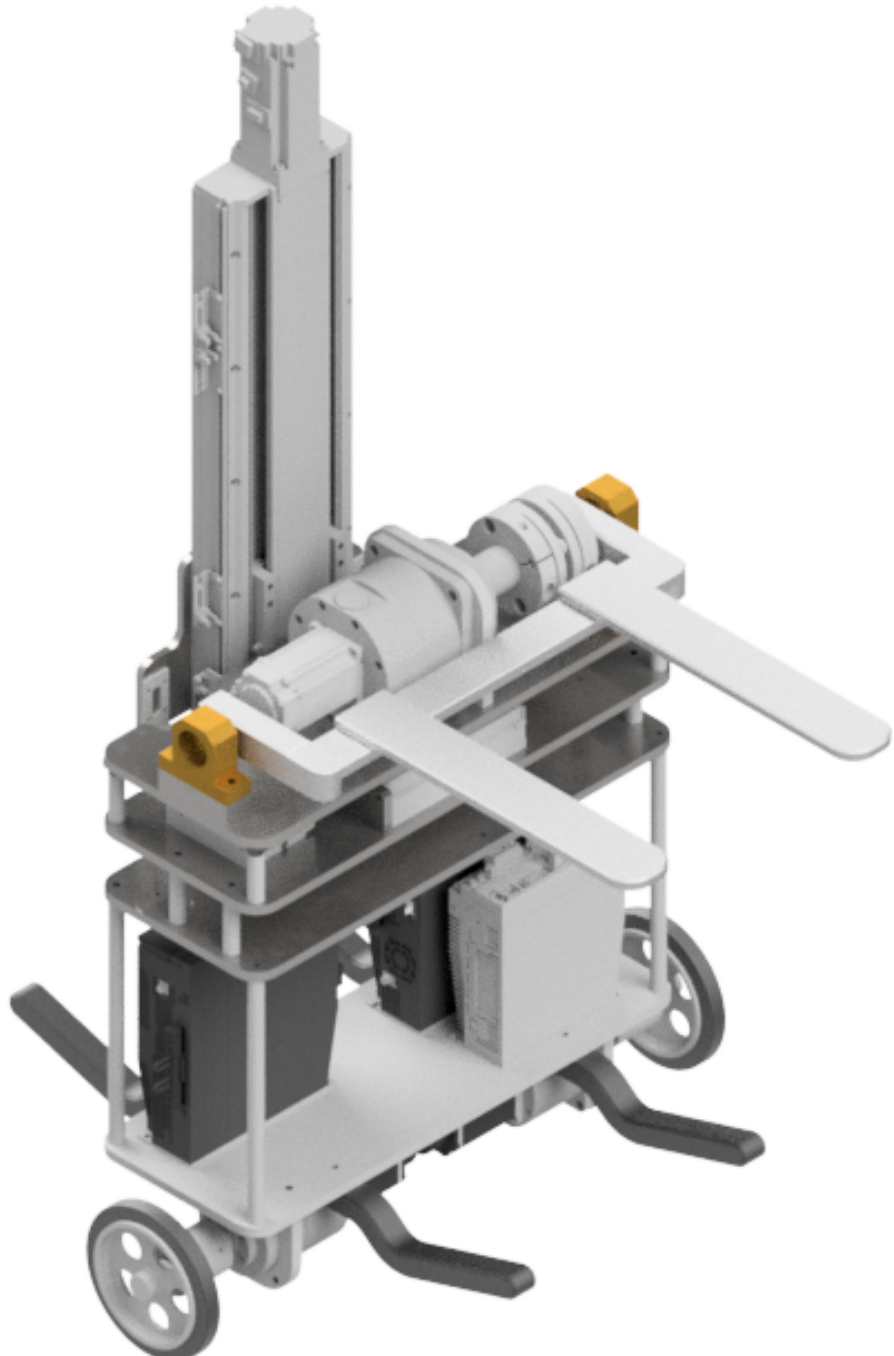
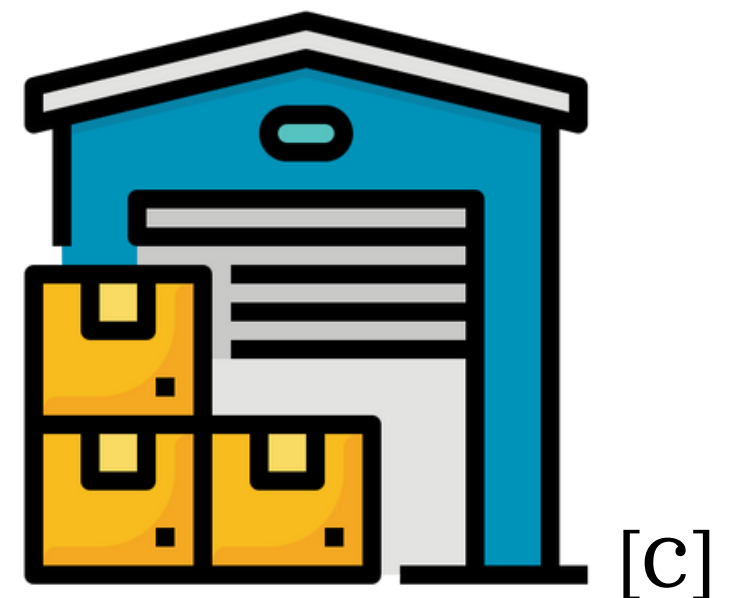
[B]



# I. Introduction

Two-Wheeled Forklift Robot:

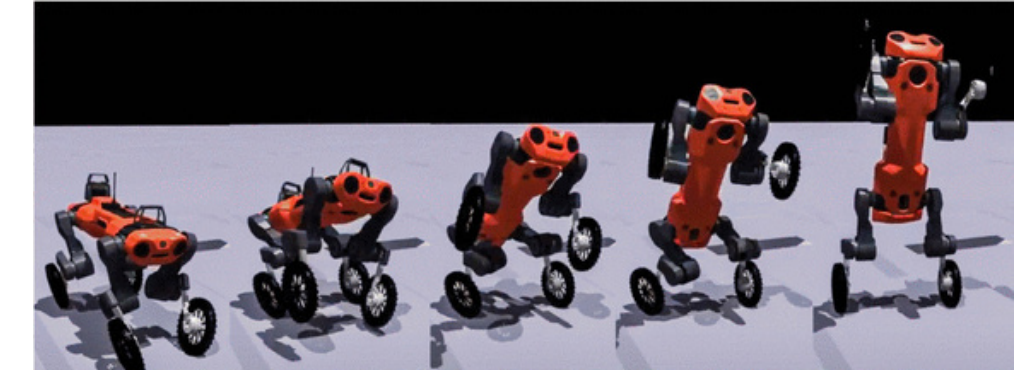
- Aimed for load movement in warehouses.
- Self-balanced mobile robot.
- Small footprint.





# I. Introduction

- Literature review





## II. Lift mechanical design

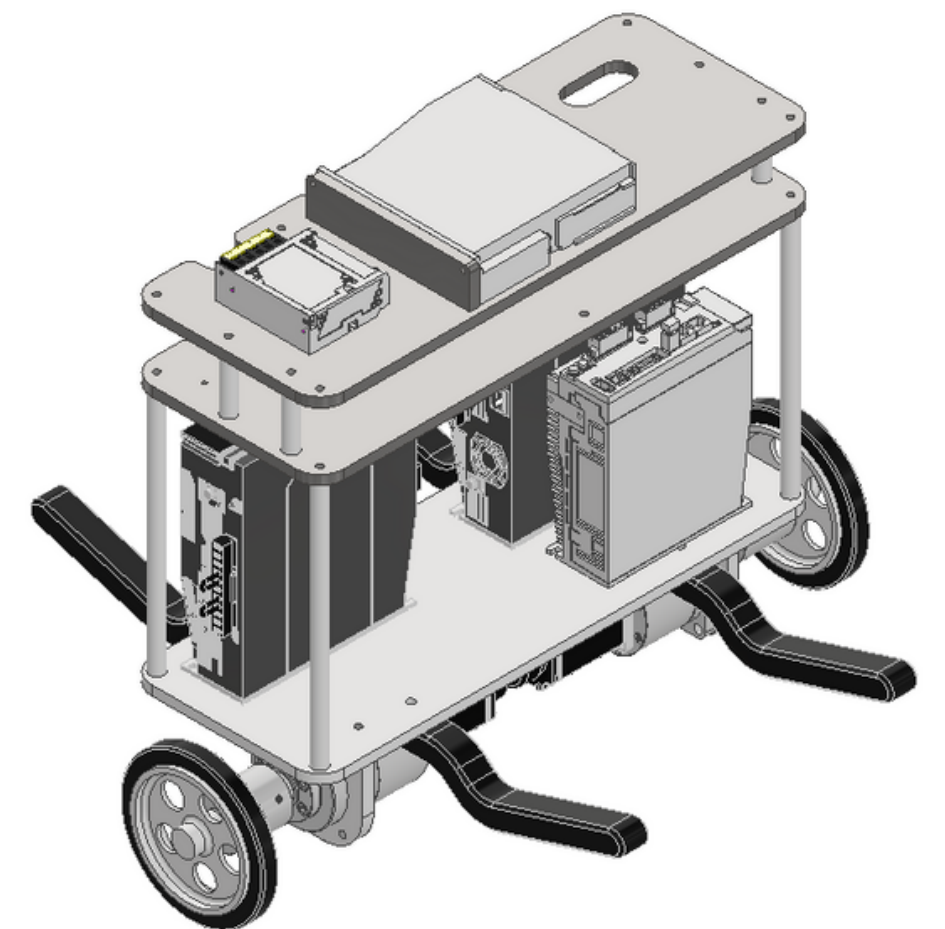
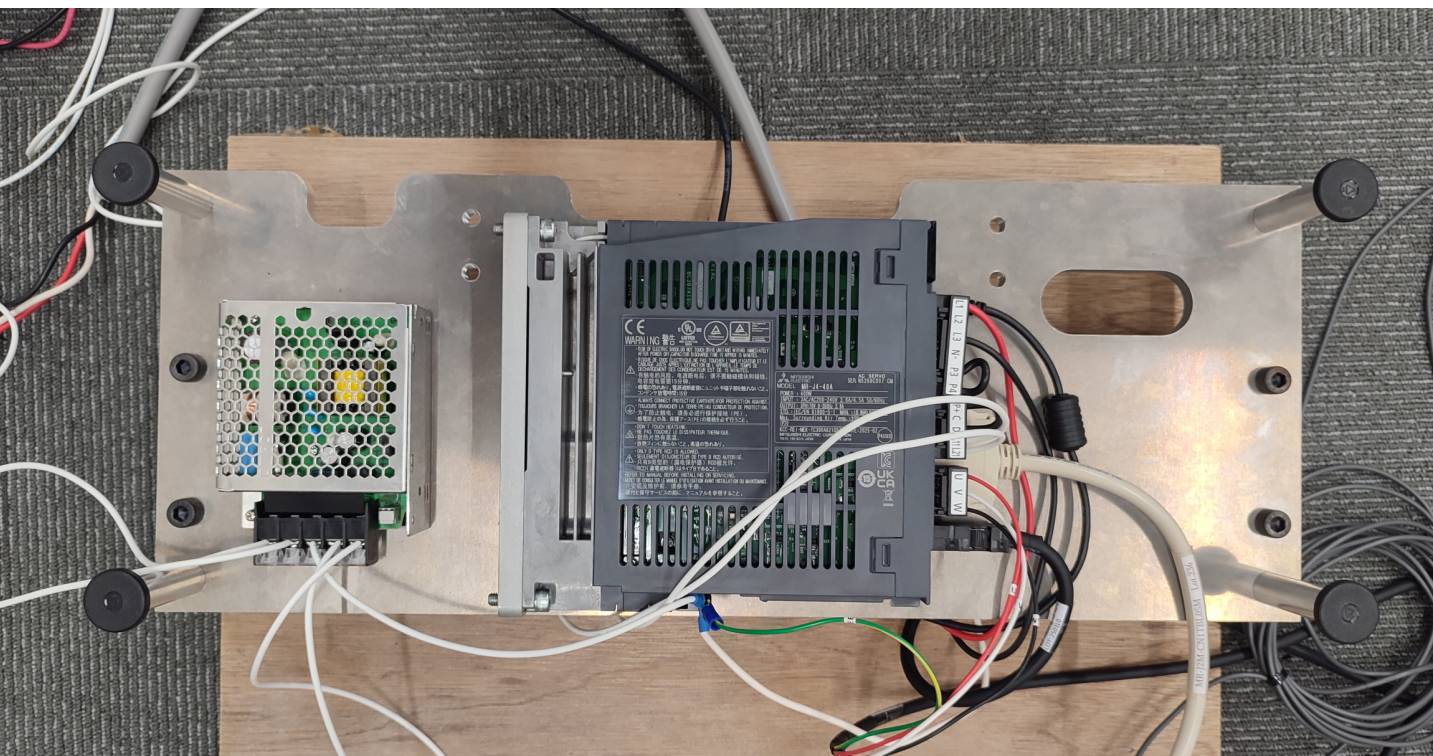
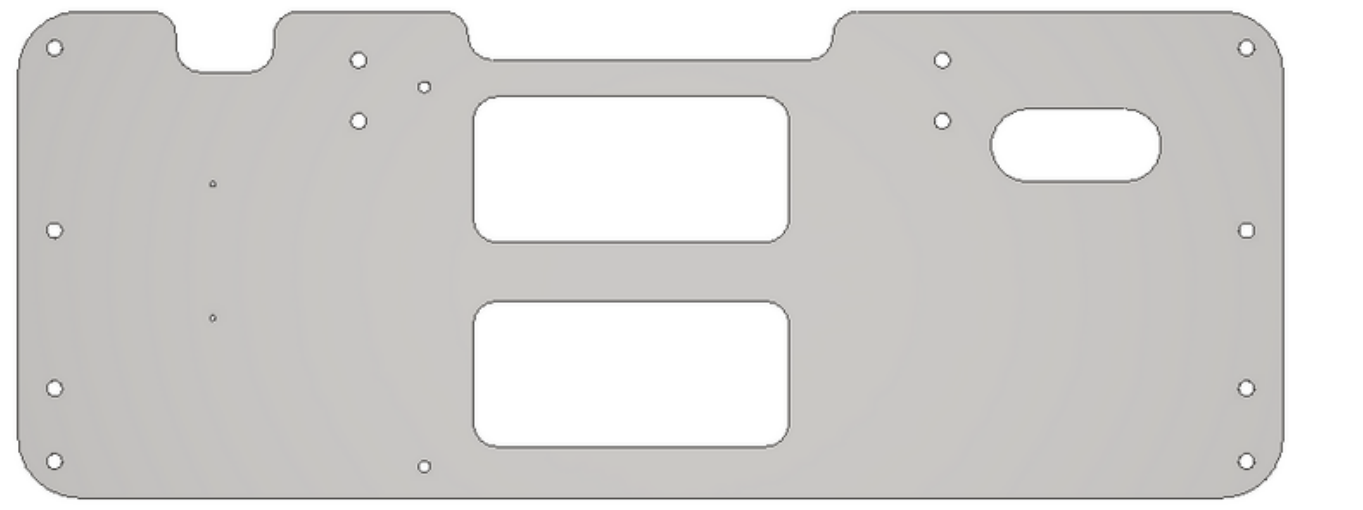
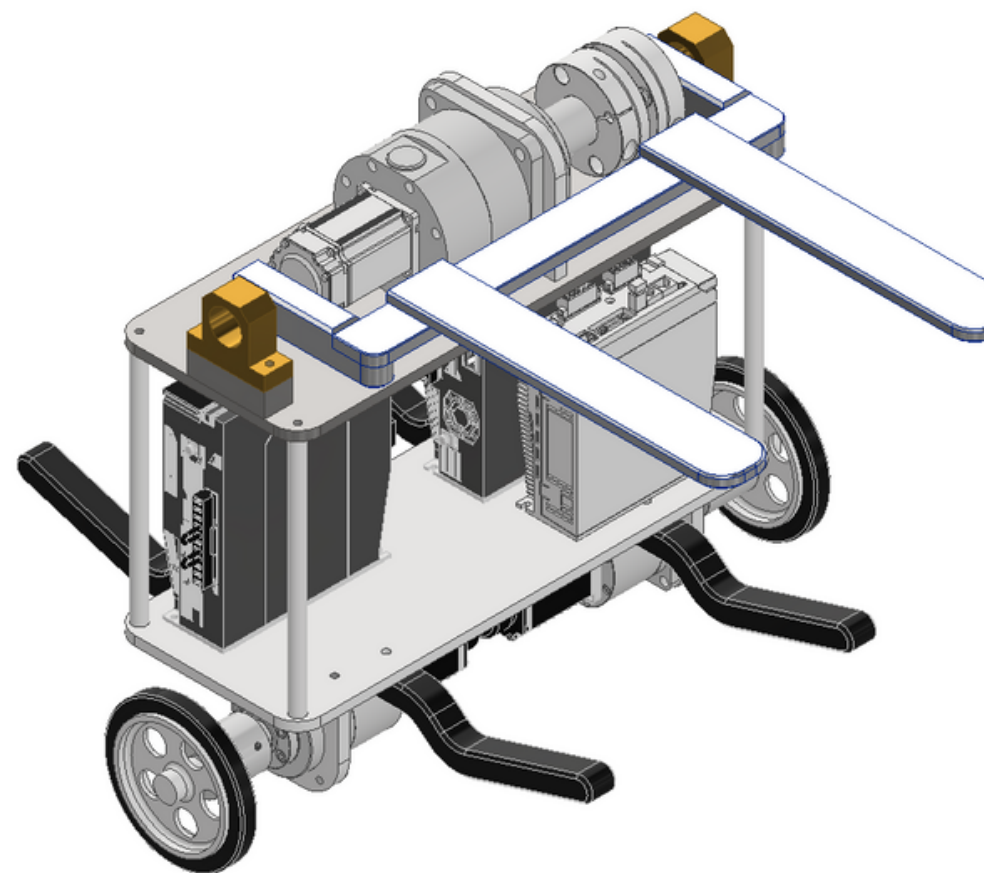
### Ball screw linear actuator ETH2-17-L5-350-BC-M40B-E5N5L

Repeatability		mm	( +/-0.005)							
Lead	mm	5	10	20	40					
Maximum Rotating Speed(mm/s)	rpm	3600	3600	3600	3600					
Maximum Linear Speed	mm/s	300	600	1200	2400					
Maximum Payload	Horizontal	kg	120	110	75	16				
	Vertical (For Non-generative power)	kg	40	25	11	9				
	Vertical(external 50W regenerative register)	Kg	50	30	18	15				
Rated Thrust	N	1389	694	347	174					
Stroke Pitch	mm	50-1200mm/50 intervals(50mm pitch)								
Maximum Acceleration	G	0.15	0.31	0.61	1.22					
Ball Screw	Basic Dynamic load rating Ca	N	13428	11223	5667	9656				
	Basic Static load rating Coa	N	29671	24456	11182	20274				
Linear Guide	Dynamic Horizontal	N	7866							
	Static Horizontal	N	78400							
Fixed Bearing	Bsic Dynamic load rating Cr	N	9666							
	Static Load rating Cor	N	6400							
AC Actuator with Motor Output	W	400								
Ball Screw	mm	C7 X ø20								
Linear Guide	mm	W15XH12.5								
Ball Screw	mm	14 X 12								
Home Sensor	Outside	T64N2(NPN)								

[19]

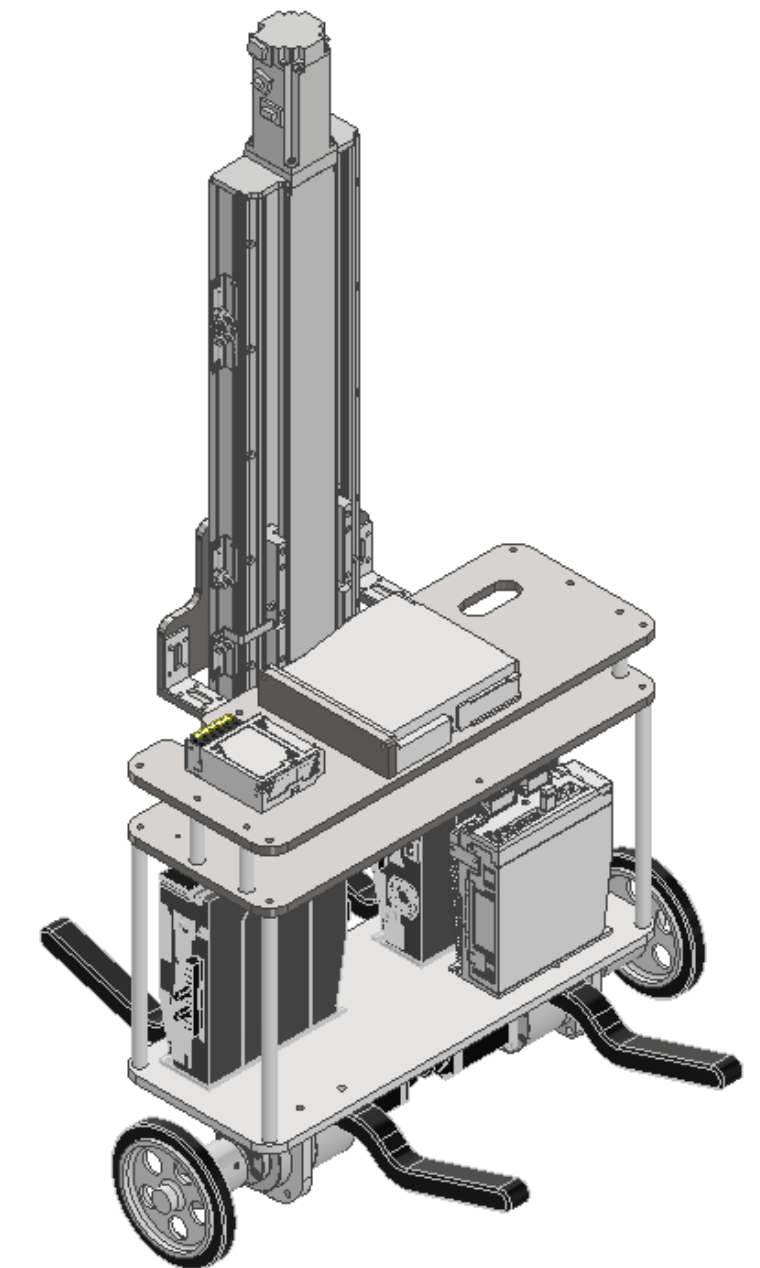
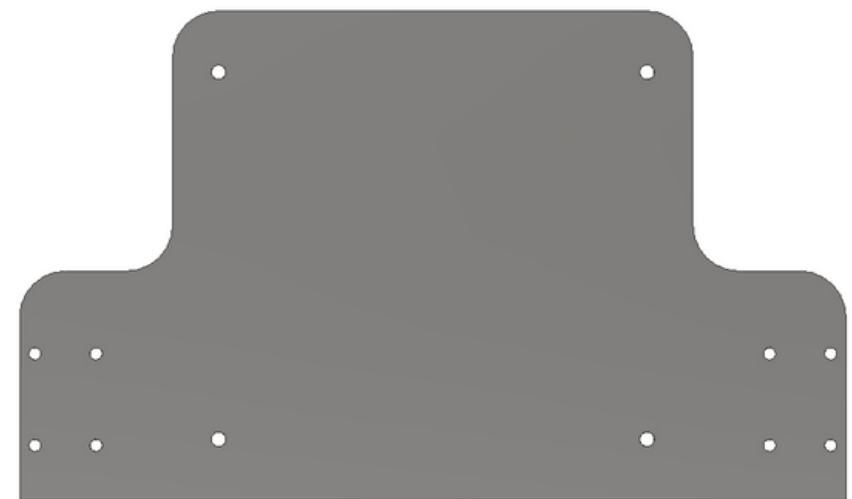
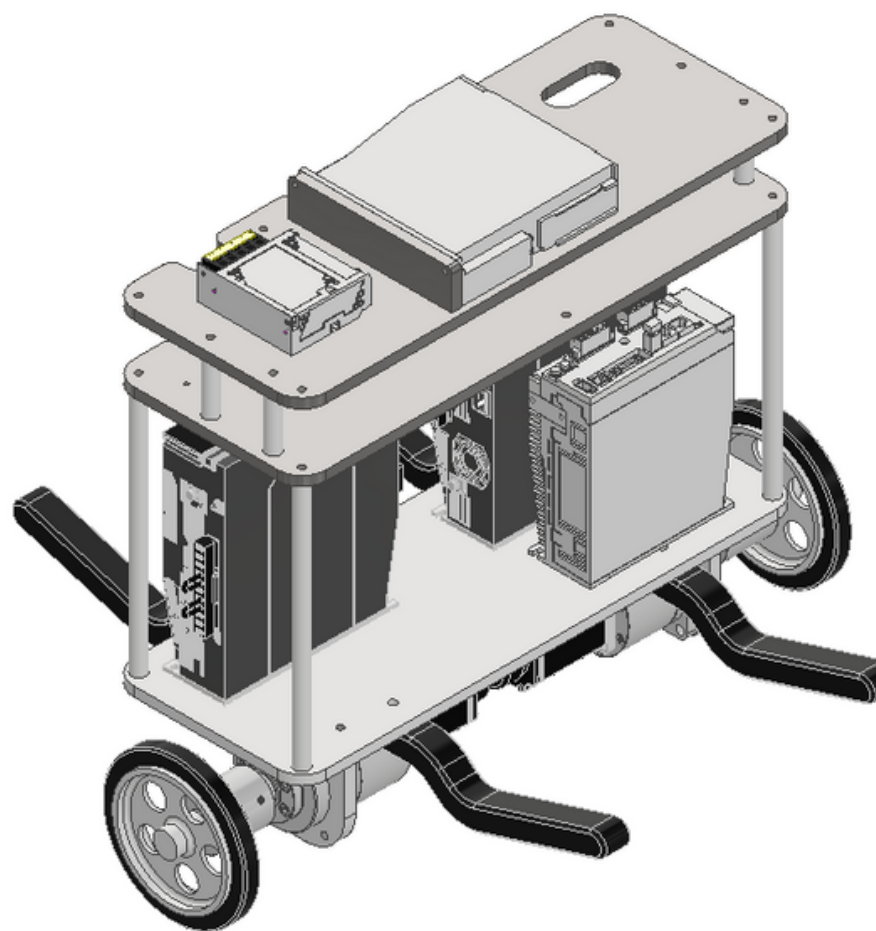


## II. Lift mechanical design



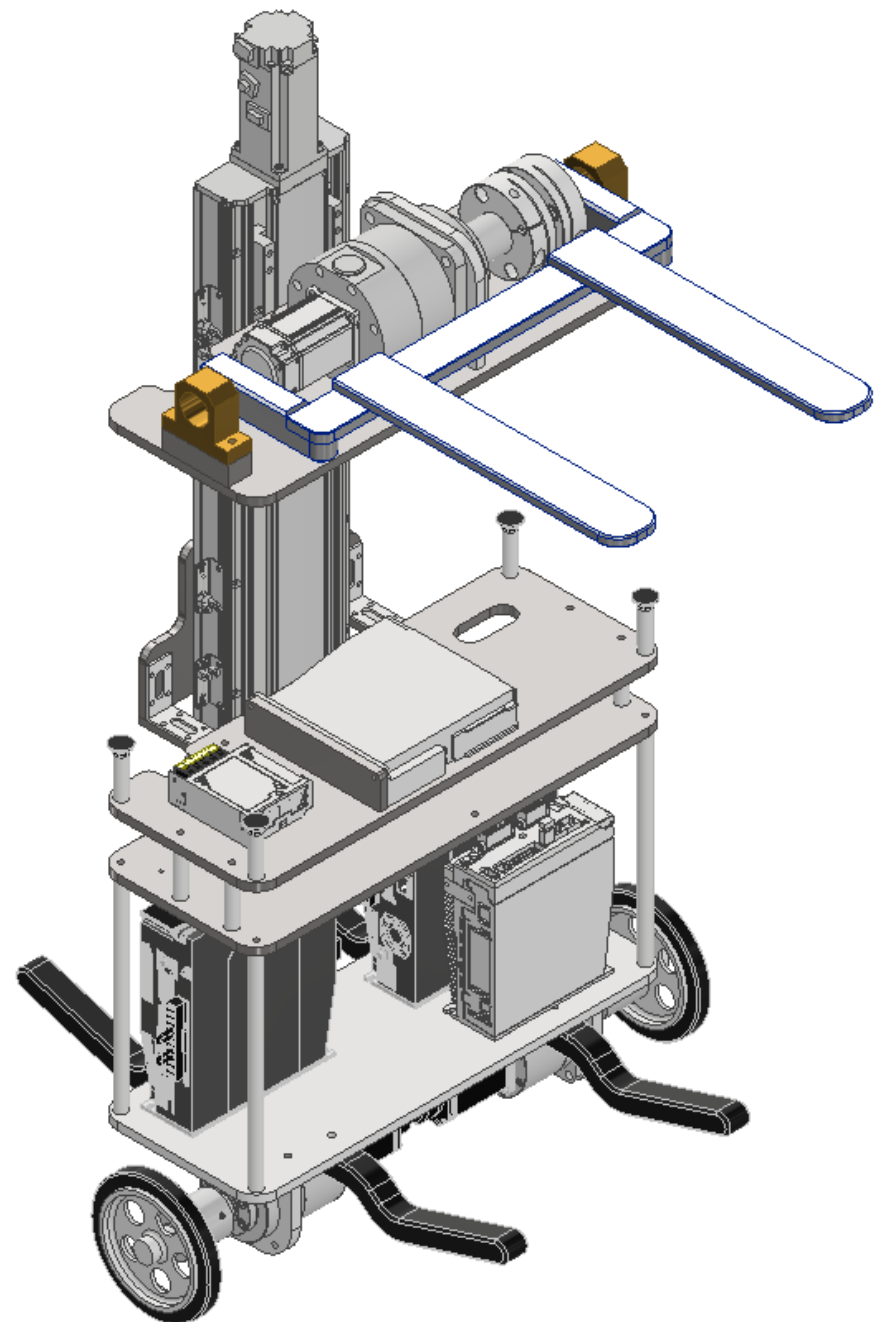
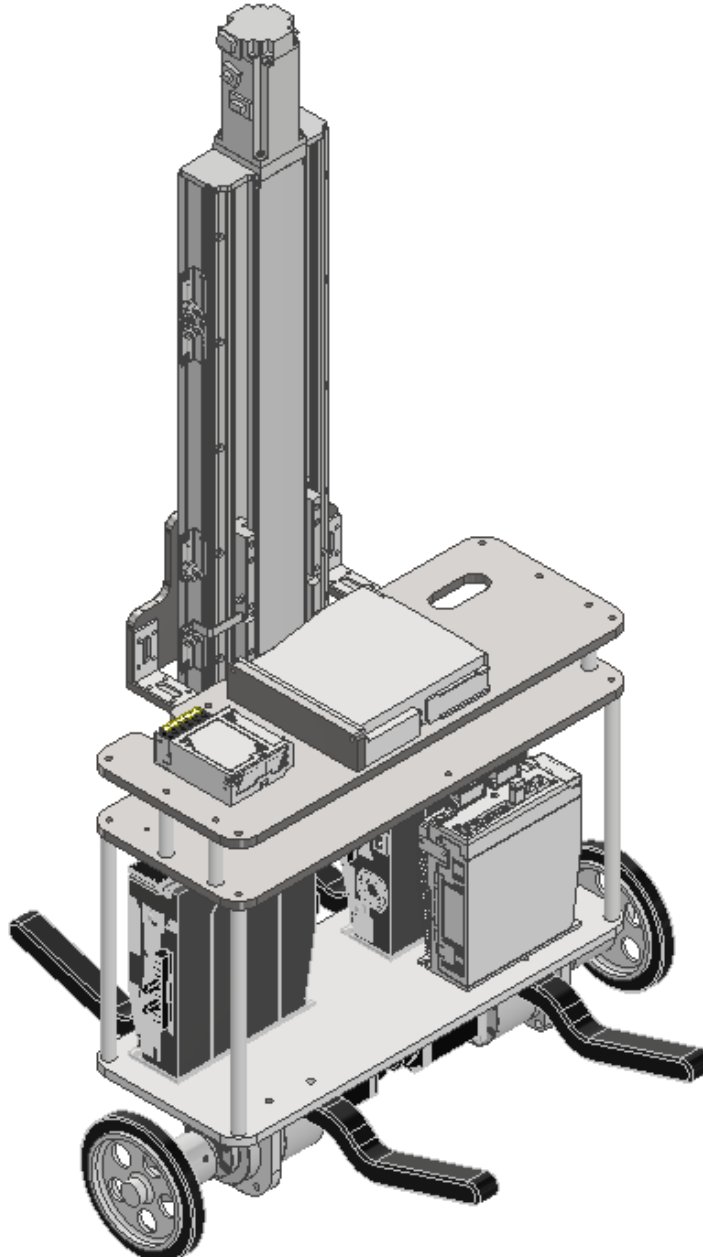


## II. Lift mechanical design





## II. Lift mechanical design



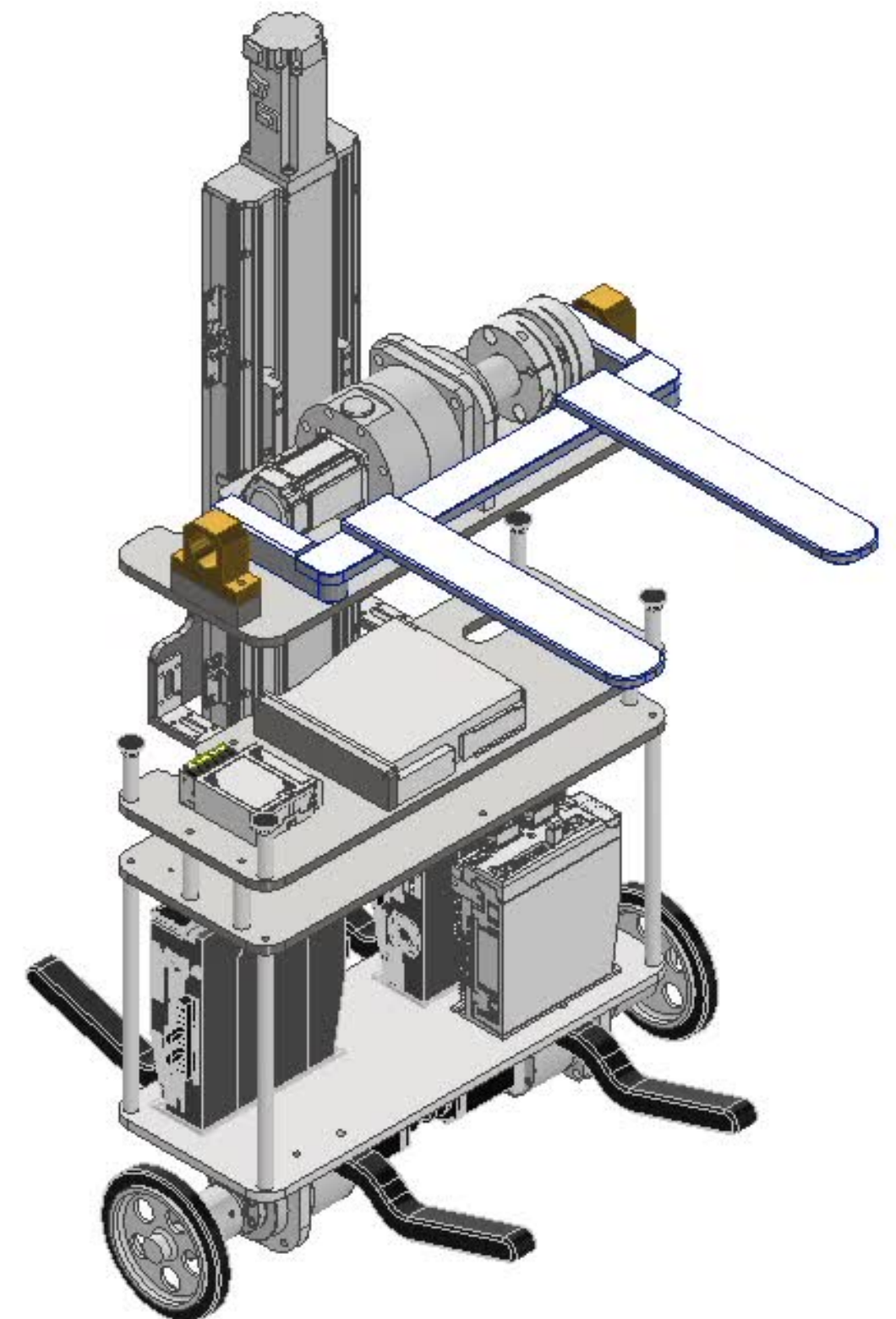


## II. Lift mechanical design

Element	Reference	Manufacturer
Wheel motors	R88M-1M40030S-S2	OMRON
Wheel reduction drives	HPG-20A-11-J6GDK	HARMONIC DRIVE
Wheels motor drivers	R88D-1SN04L-ECT	OMRON
Fork motor	R88M-K40030S	OMRON
Fork reduction drive	HPG-32A-33-J2NELA	HARMONIC DRIVE
Fork motor driver	R88D-KN04L-ECT	OMRON
Lift motor	HG-KR43B	MITSUBISHI
Lift mechanism	ETH2-17-L5-350	TOYO ROBOTICS
Lift motor driver	MR-J4-40TM-ECT	MITSUBISHI

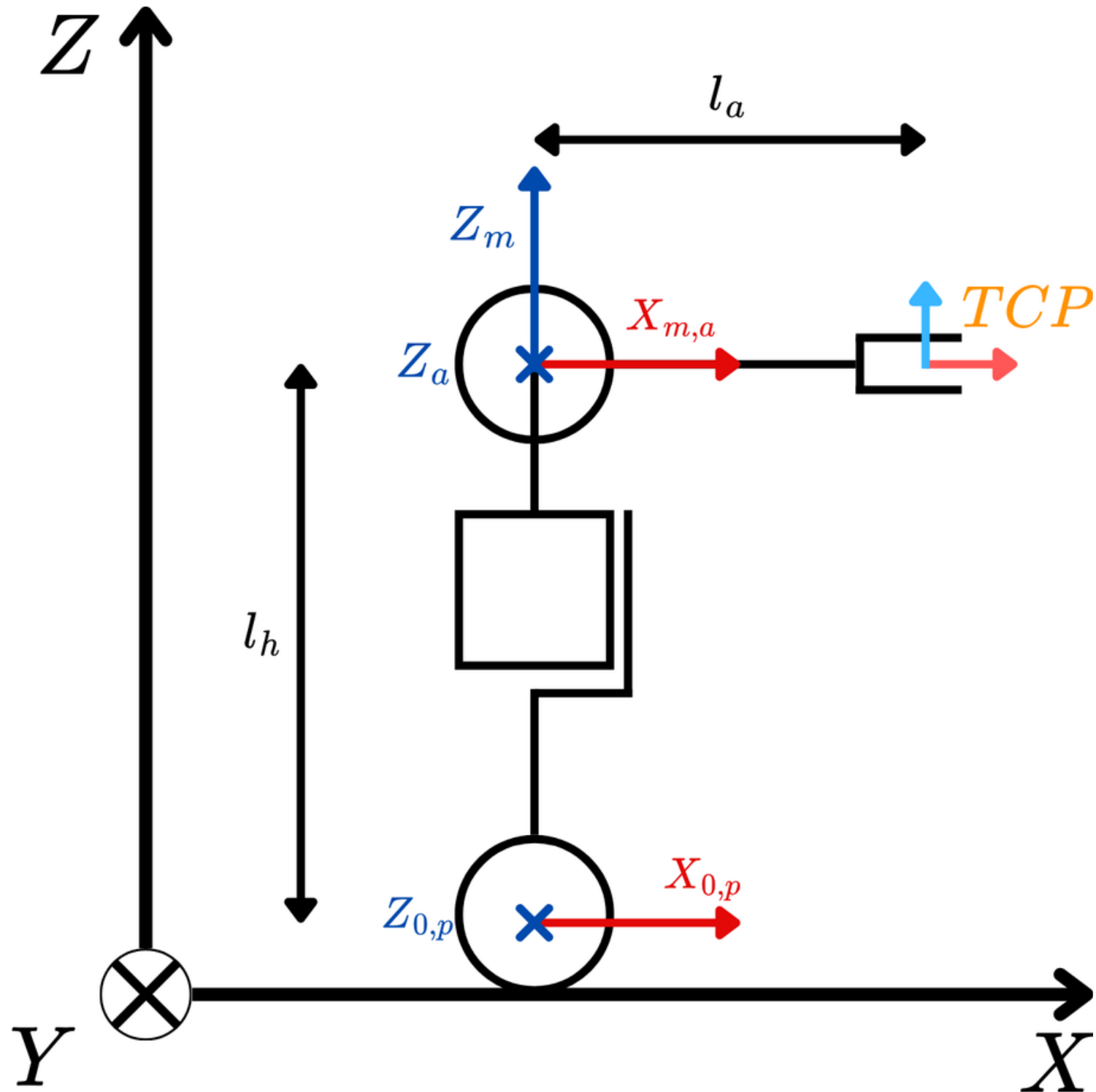


## II. Lift mechanical design





### III. Modeling



Kinematics:

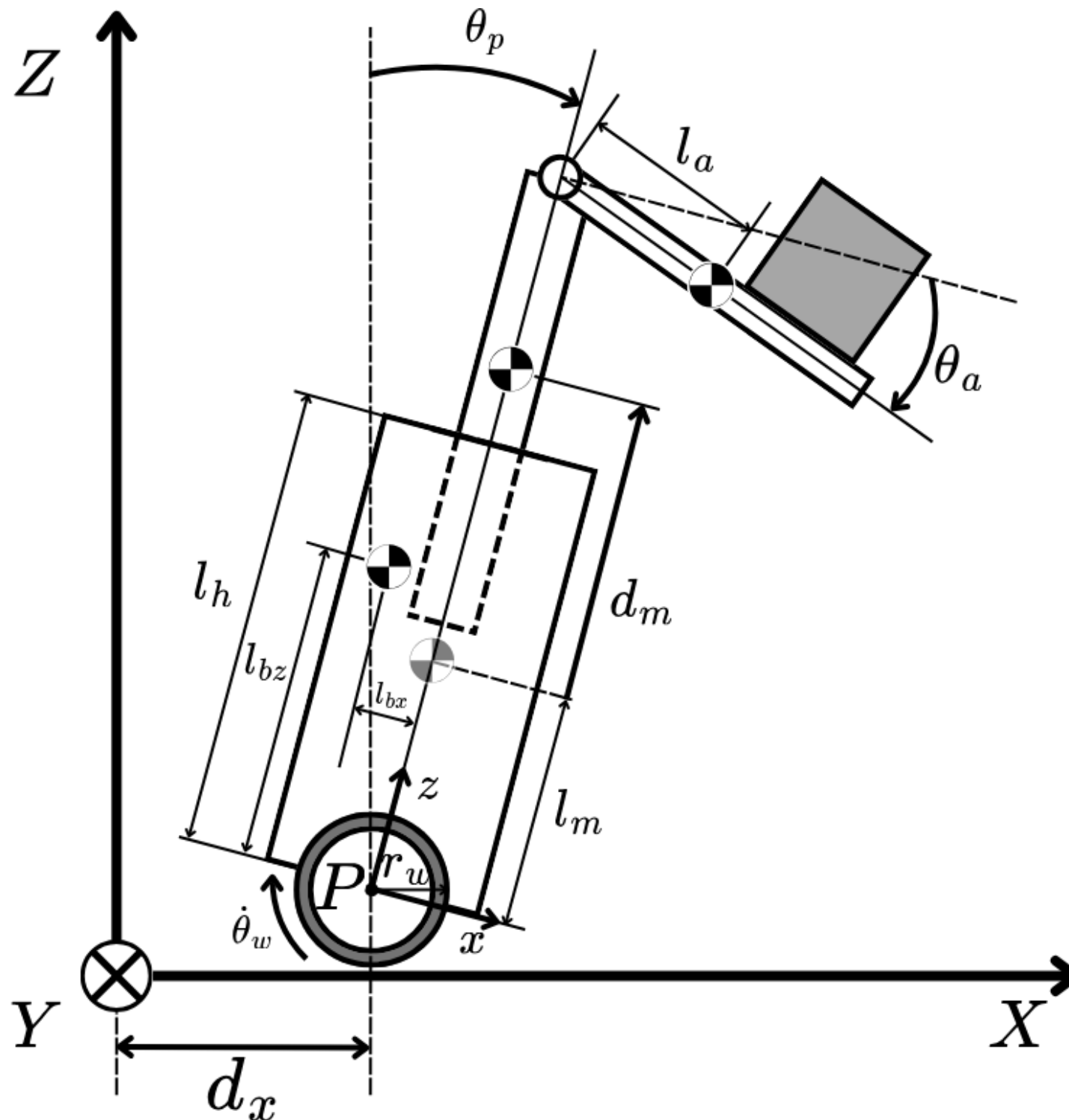
$\theta_w$  : Wheel angle,    $\theta_p$  : Pitch angle,  
 $d_m$  : Lift displacement,    $\theta_a$  : Arm angle

$$\theta_p + \theta_a = 0$$

$$H_T^B = \begin{pmatrix} 1 & 0 & 0 & s_p(l_h + d_m) + l_a \\ 0 & 1 & 0 & 0 \\ 0 & 0 & 1 & r_w + c_p(l_h + d_m) \\ 0 & 0 & 0 & 1 \end{pmatrix}$$



### III. Modeling



Kinematics:

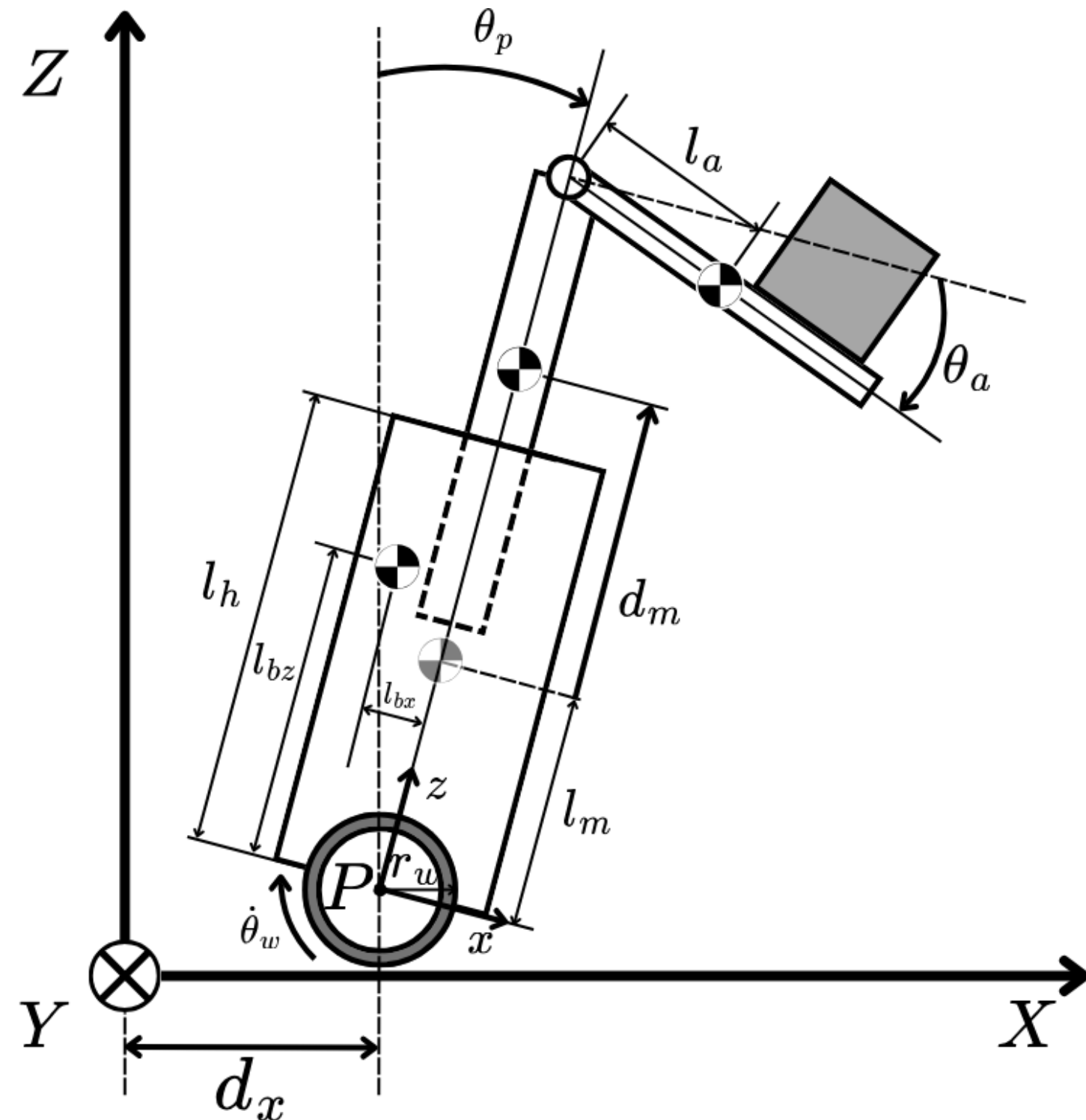
$$CoG = \left( \begin{array}{c} \frac{m_l \left( d_m s_p + l_h s_p + \frac{t_1}{g m_l} \right) + m_a (l_a + d_m s_p + l_h s_p) + m_b (l_{bz} s_p - l_{bx} c_p) + m_m (d_m + l_m) s_p}{m_a + m_b + m_l + m_m} \\ \frac{(m_a + m_l) (d_m c_p + l_h c_p) + m_b (l_{bz} c_p + l_{bx} s_p) + m_m (d_m + l_m) c_p}{m_a + m_b + m_l + m_m} \end{array} \right)$$

❖

$$\begin{cases} r_w + c_p(l_h + d_m) = z \\ c_p \dot{d}_m - s_p(l_h + d_m) \dot{\theta}_p = \dot{z} \\ CoG_x(\theta_p, d_m, m_l, t_1) = \sin(\theta_t) l_t \\ \dot{\theta}_p = 0 \end{cases}$$



### III. Modeling



Dynamics:

$$M(q)\ddot{q} + H(\dot{q}, q) + G(q) = \tau$$

Generalized coordinates:

$$q = [\theta_w \quad \theta_p \quad d_m \quad \theta_a]^T$$

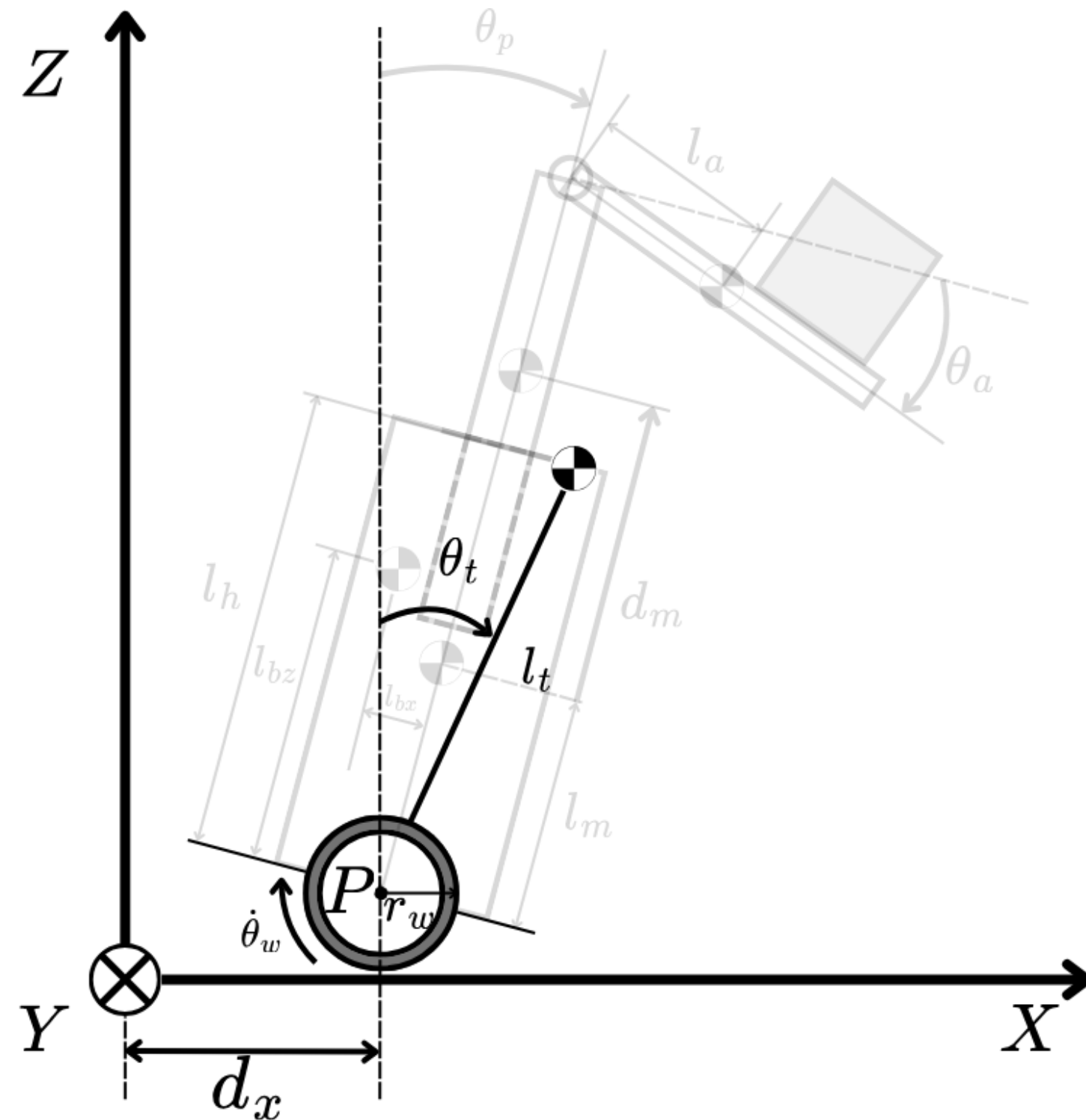
$$\tau = [n_w\tau_w \quad -n_w\tau_w \quad f_m \quad n_a\tau_a]^T$$

$\tau_w$  : Wheel torque,  $f_m$  : Lift force,

$\tau_a$  : Arm torque



### III. Modeling



Simplified dynamics:

❖  $M^*(q')\ddot{q}' + H^*(\dot{q}', q') + G^*(q') = \tau^*(\ddot{x})$

Generalized coordinates:

$$q' = [\theta_w \quad \theta_t]^T$$

$$\tau^*(\ddot{x}) = [n_w \tau_w(\ddot{x}) \quad -n_w \tau_w(\ddot{x})]^T$$

$$\tau_w(\ddot{x}) = r_w m_t \ddot{x}^{ref}$$



$$\theta_t = \text{atan}\left(\frac{CoG_x}{CoG_z}\right), \quad l_t = \|CoG\|$$



## IV. Control

Synthesized Pitch Angle Disturbance Observer (SPADO):

$$m_{11}\ddot{\theta}_w + m_{12}\ddot{\theta}_p + m_{13}\ddot{d}_m + m_{14}\ddot{\theta}_a + h_1 = n_w\tau_w - T_{lw}$$

$$m_{n11}\ddot{\theta}_w^{res} = n_w\tau_w^{ref} - \tilde{\tau}_w^{dist}$$

$$\tilde{\tau}_w^{dist} = (m_{11} - m_{n11})\ddot{\theta}_w + m_{12}\ddot{\theta}_p + m_{13}\ddot{d}_m + m_{14}\ddot{\theta}_a + h_1 + T_{lw}$$

$$m_{21}\ddot{\theta}_w + m_{22}\ddot{\theta}_p + m_{23}\ddot{d}_m + m_{24}\ddot{\theta}_a + h_2 + g_2 = -n_w\tau_w - T_{lp}$$

$$m_{n21}\ddot{\theta}_w^{res} + m_{n22}\ddot{\theta}_p^{res} = -n_w\tau_w^{ref} - \tilde{\tau}_p^{dist}$$

$$\tilde{\tau}_p^{dist} = (m_{21} - m_{n21})\ddot{\theta}_w + (m_{22} - m_{n22})\ddot{\theta}_p + m_{23}\ddot{d}_m + m_{24}\ddot{\theta}_a + h_2 + g_2 + T_{lp}$$



# IV. Control

SPADO:

$$m_{n22}\ddot{\theta}_p^{res} + \frac{m_{n21} + m_{n11}}{m_{n11}}n_w\tau_w^{ref} = \frac{m_{n21}}{m_{n11}}\tilde{\tau}_w^{dis} - \tilde{\tau}_p^{dist}$$

$$\tilde{\tau}_s^{dist} = \tilde{\tau}_p^{dist} - \frac{m_{n21}}{m_{n11}}\tilde{\tau}_w^{dis}$$

$$m_{n22}\ddot{\theta}_p^{res} + \frac{m_{n21} + m_{n11}}{m_{n11}}n_w\tau_w^{ref} = -\tilde{\tau}_s^{dist}$$

$$\hat{\tau}_s^{dist} = \frac{g_s}{s + g_s}(g_s m_{n22}\dot{\theta}_p^{res} - \frac{m_{n21} + m_{n11}}{m_{n11}}n_w\tau_w^{ref}) - g_s m_{n22}\dot{\theta}_p^{res}$$

Pseudo differentiation



## IV. Control

PD controller pitch angle:

$$V = \frac{1}{2}K_1(\theta_p^{cmd} - \theta_p^{res})^2 + \frac{1}{2}K_2(\dot{\theta}_p^{cmd} - \dot{\theta}_p^{res})^2$$

$$\dot{V} = (\dot{\theta}_p^{cmd} - \dot{\theta}_p^{res})(K_1(\theta_p^{cmd} - \theta_p^{res}) + K_2(\ddot{\theta}_p^{cmd} - \boxed{\ddot{\theta}_p^{res}}))$$

$$\dot{V} = -K_3(\dot{\theta}_p^{cmd} - \dot{\theta}_p^{res})^2$$

$$\tau_w^{ref} = -\frac{m_{n11}m_{n22}}{n_w(m_{n21} + m_{n11})} \left( K_{pp}(\boxed{\theta_p^{cmd}} - \theta_p^{res}) + K_{dp}(\boxed{\dot{\theta}_p^{cmd}} - \dot{\theta}_p^{res}) + \boxed{\ddot{\theta}_p^{cmd}} \right) - \frac{m_{n11}}{n_w(m_{n21} + m_{n11})} \boxed{\hat{\tau}_s^{dist}}$$

$$K_{pp} = \frac{K_1}{K_2}, \quad K_{dp} = \frac{K_3}{K_2}$$



## IV. Control

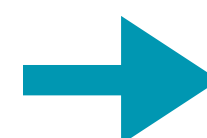
Fork Disturbance Observer (FDOB):

$$m_{41}\ddot{\theta}_w + m_{42}\ddot{\theta}_p + m_{43}\ddot{d}_m + m_{44}\ddot{\theta}_a + h_4 + g_4 = n_a\tau_a - T_{la}$$

$$m_{n44}\ddot{\theta}_a^{res} = n_a\tau_a^{ref} - \tilde{\tau}_a^{dist}$$

$$\tilde{\tau}_a^{dist} = m_{41}\ddot{\theta}_w^{res} + m_{42}\ddot{\theta}_p^{res} + m_{43}\ddot{d}_m^{res} + (m_{44} - m_{n44})\ddot{\theta}_a^{res} + h_4 + g_4 + T_{la}$$

$$\hat{\tau}_a^{dist} = \frac{g_a}{s + g_a}(n_a\tau_a^{ref} + g_a m_{n44}\dot{\theta}_a^{res}) - g_a m_{n44}\dot{\theta}_a^{res}$$



Pseudo differentiation

PD controller fork angle:

$$\tau_a^{ref} = K_{pa}(\theta_a^{cmd} - \theta_a^{res}) + K_{da}(\dot{\theta}_a^{cmd} - \dot{\theta}_a^{res}) + \hat{\tau}_a^{dist}$$



## IV. Control

Fork Reaction Torque Observer (FRTOB):

$$T_{la} = \tilde{\tau}_a^{ext} + \tilde{\tau}_a^{fric}$$

$$\tilde{\tau}_a^{reac} = m_{41}\ddot{\theta}_w^{res} + m_{42}\ddot{\theta}_p^{res} + m_{43}\ddot{d}_m^{res} + (m_{44} - m_{n44})\ddot{\theta}_a^{res} + h_4 + \tilde{\tau}_a^{ext}$$

$$m_{n44}\ddot{\theta}_a^{res} = n_a \tau_a^{ref} - g_4 - \tilde{\tau}_a^{fric} - \tilde{\tau}_a^{reac}$$

$$\hat{\tau}_a^{reac} = \frac{g_r}{s + g_r} (n_a \tau_a^{ref} + g_r m_{n44} \dot{\theta}_a^{res} - g_4 - \tilde{\tau}_a^{fric}) - g_r m_{n44} \dot{\theta}_a^{res}$$

Pseudo differentiation

$$t_1 = -\hat{\tau}_a^{reac}$$



# IV. Control

Lift Disturbance Observer (LDOB):

$$m_{31}\ddot{\theta}_w + m_{32}\ddot{\theta}_p + m_{33}\ddot{d}_m + m_{34}\ddot{\theta}_a + h_3 + g_3 = f_m - F_{lm}$$

$$m_{n33}\ddot{d}_m^{res} = f_m^{ref} - \tilde{f}_m^{dist}$$

$$\tilde{f}_m^{dist} = m_{31}\ddot{\theta}_w^{res} + m_{32}\ddot{\theta}_p^{res} + (m_{33} - m_{n33})\ddot{d}_m^{res} + m_{34}\ddot{\theta}_a^{res} + h_3 + g_3 + F_{lm}$$

$$\hat{f}_m^{dist} = \frac{g_m}{s + g_m}(f_m^{ref} + g_m m_{n33} \dot{d}_m^{res}) - g_m m_{n33} \dot{d}_m^{res} \rightarrow \text{Pseudo differentiation}$$

PD controller lift displacement:

$$f_m^{ref} = K_{pm}(d_m^{cmd} - d_m^{res}) + K_{dm}(\dot{d}_m^{cmd} - \dot{d}_m^{res}) + \hat{f}_m^{dist}$$



# IV. Control

Lift Reaction Force Observer (LRFOB):

$$F_{lm} = \tilde{f}_m^{ext} + \tilde{f}_m^{fric}$$

$$\tilde{f}_m^{reac} = m_{31}\ddot{\theta}_w^{res} + m_{32}\ddot{\theta}_p^{res} + (m_{33} - m_{n33})\ddot{d}_m^{res} + m_{34}\ddot{\theta}_a^{res} + h_3 + \tilde{f}_m^{ext}$$

$$m_{n44}\ddot{d}_m^{res} = f_m^{ref} - g_3 - \tilde{f}_m^{fric} - \tilde{f}_m^{reac}$$

$$\hat{f}_m^{reac} = \frac{g_r}{s + g_r} (f_m^{ref} + g_r m_{n33} \dot{d}_m^{res} - g_3 - \tilde{f}_m^{fric}) - g_r m_{n33} \dot{d}_m^{res}$$

Pseudo differentiation

$$m_l = \frac{\hat{f}_m^{reac}}{g \cos(\theta_p)}$$



## IV. Control

Wheel Position Control:

$$\theta_p^{cmd-PD} = K_{pw}(\theta_w^{cmd} - \theta_w^{res}) + K_{dw}(\dot{\theta}_w^{cmd} - \dot{\theta}_w^{res})$$

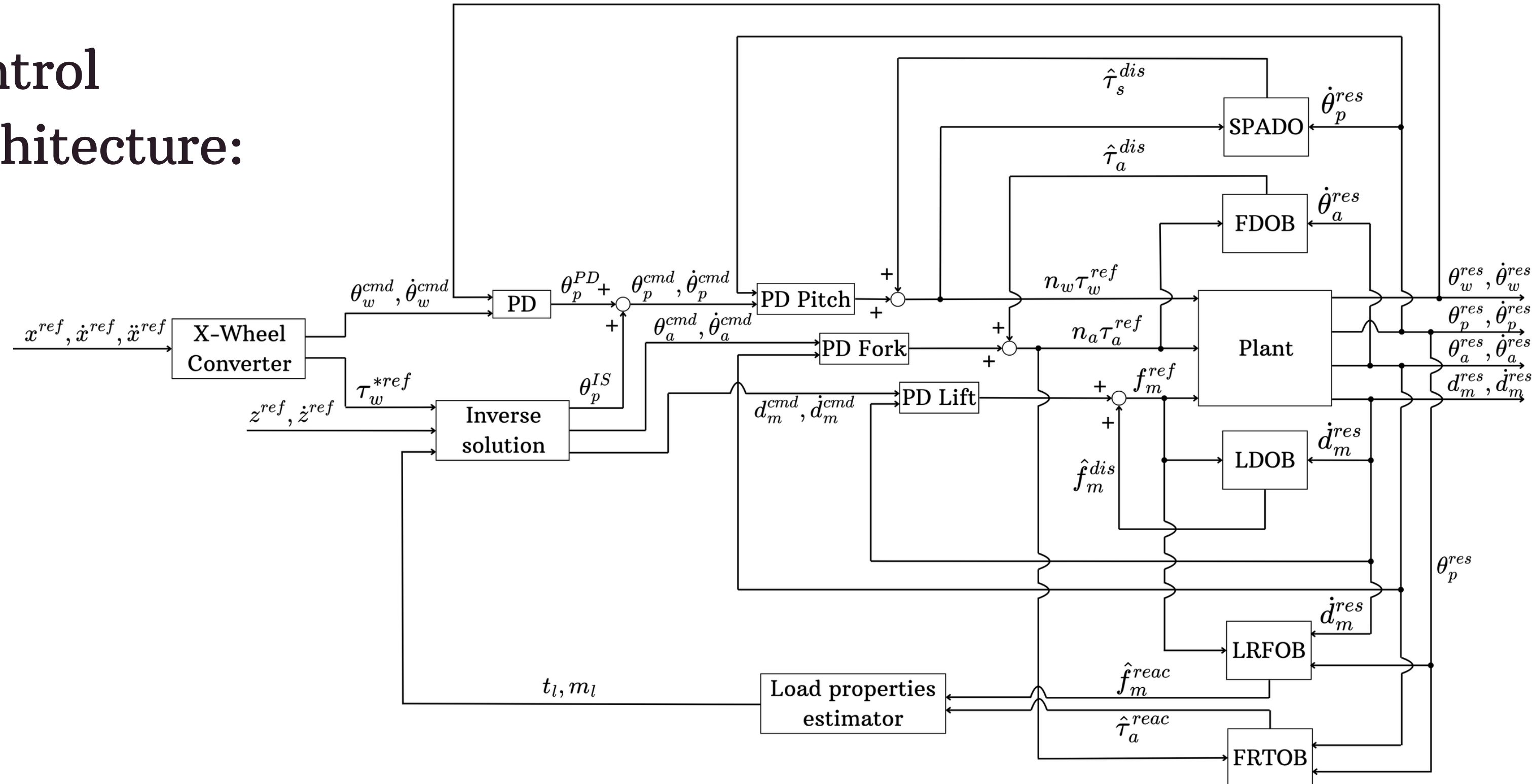
Total pitch command:

$$\theta_p^{cmd} = \theta_p^{cmd-IS} + \theta_p^{cmd-PD}$$



# IV. Control

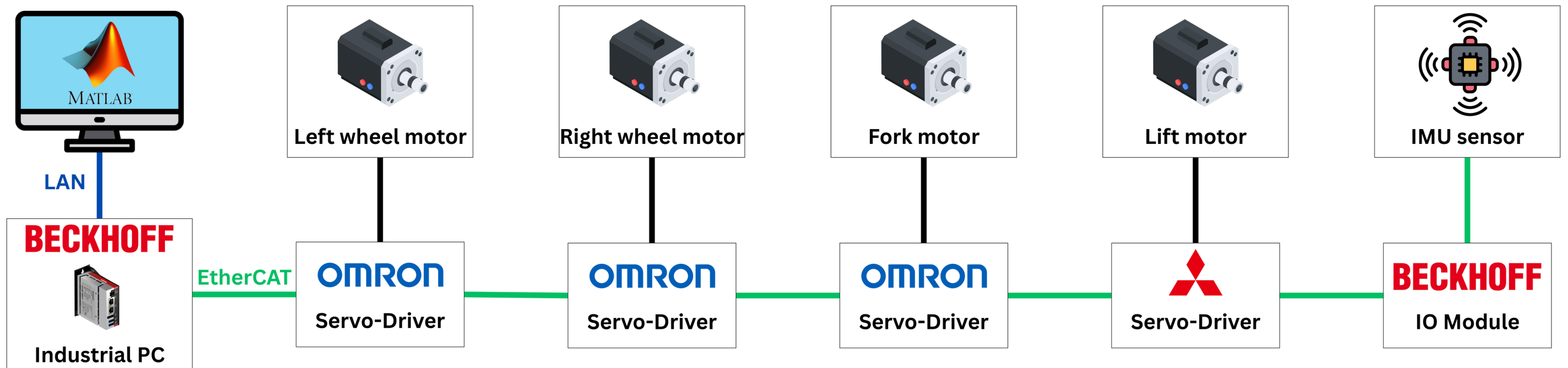
## Control Architecture:





# IV. Control

Physical implementation:





# V. Results

<b>Parameter</b>	<b>Explanation</b>	<b>Value</b>
$K_{pp}$	P-gain of pitch angle control	200
$K_{pd}$	D-gain of pitch angle control	50
$K_{pa}$	P-gain of arm position control	200
$K_{da}$	D-gain of arm position control	50
$K_{pm}$	P-gain of lift position control	200
$K_{dm}$	D-gain of lift position control	50
$K_{pw}$	P-gain of wheel position control	0.07
$K_{dw}$	D-gain of wheel position control	0.09
$g_s$ (rad/s)	Cutoff angular frequency of SPADO	$2\pi 6$
$g_a$ (rad/s)	Cutoff angular frequency of arm FDOB	$2\pi 5$
$g_r$ (rad/s)	Cutoff angular frequency of FRTOB, LRFOB	$2\pi 1$
$g_m$ (rad/s)	Cutoff angular frequency of LDOB	$2\pi 4$
$N_w$	Wheel gear ratio	11
$N_a$	Arm gear ratio	33

<b>Parameter</b>	<b>Explanation</b>	<b>Value</b>
$I_{wy}$ ( $\text{kg m}^2$ )	Wheel inertia	0.0052
$I_{by}$ ( $\text{kg m}^2$ )	Body inertia	4.0590
$I_{my}$ ( $\text{kg m}^2$ )	Lift inertia	0.0482
$I_{ay}$ ( $\text{kg m}^2$ )	Arm inertia	0.0890
$l_{bz}$ (m)	Body CoG z coordinate	0.3206
$l_{bx}$ (m)	Body CoG x coordinate	0.0246
$l_m$ (m)	Lift CoG distance	0.3975
$l_a$ (m)	Arm CoG distance	0.2200
$m_w$ (kg)	Wheel mass	1.21
$m_b$ (kg)	Body mass	64.1
$m_m$ (kg)	Lift mass	21.5
$m_a$ (kg)	Arm mass	3.5
$m_l$ (kg)	Load mass	5



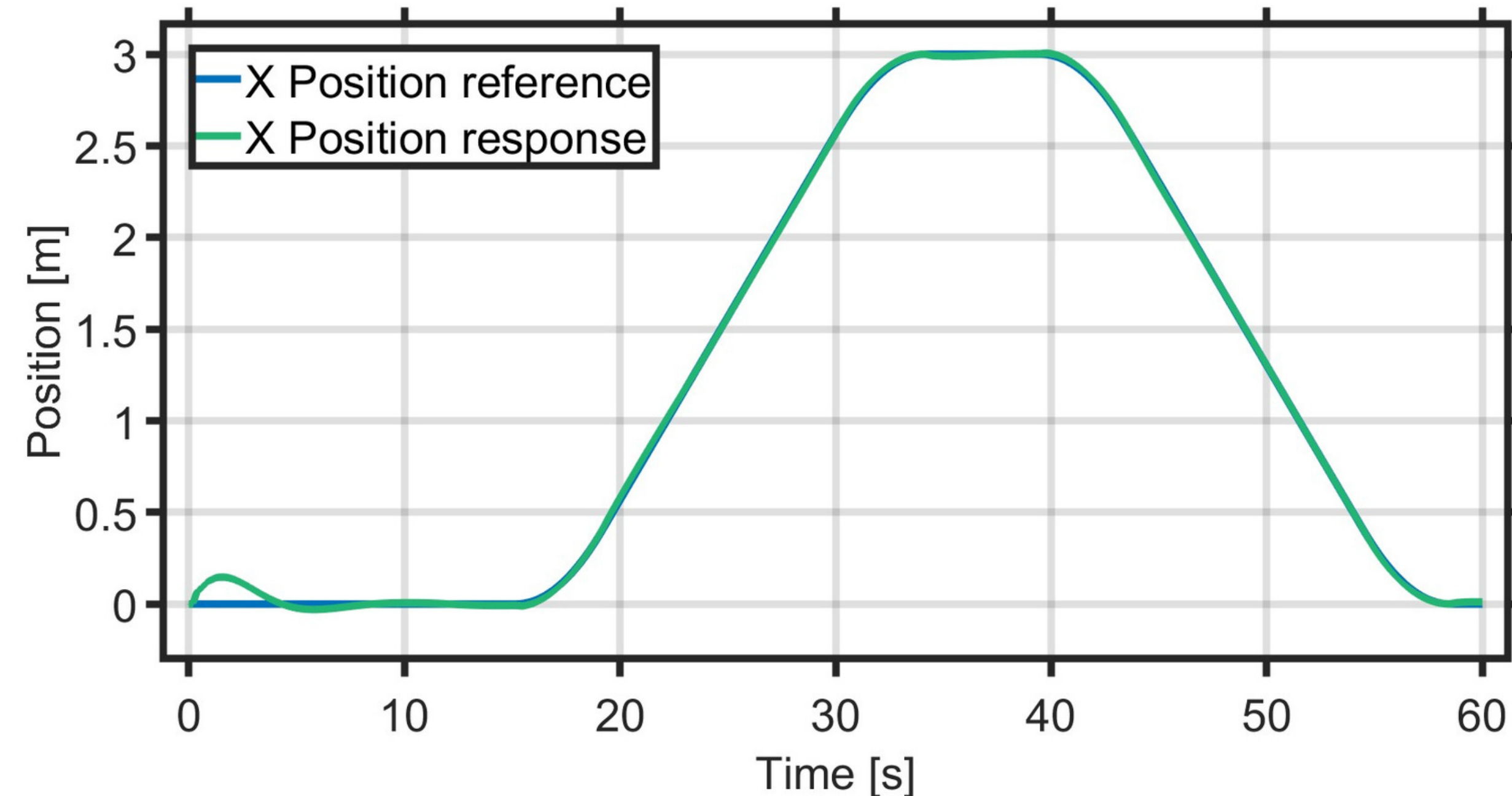
# V. Simulation





# V. Simulation

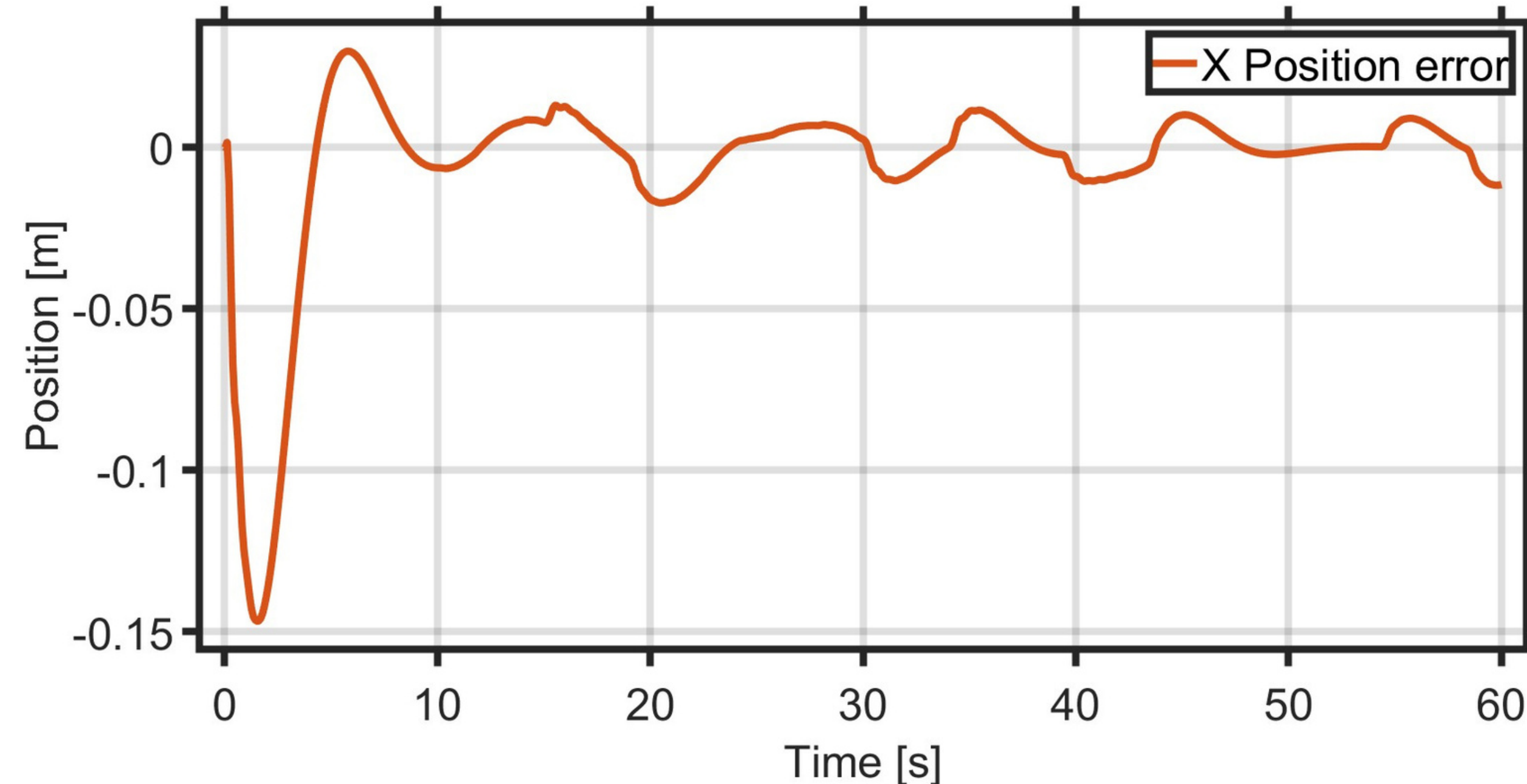
## Horizontal displacement of the robot





## V. Simulation

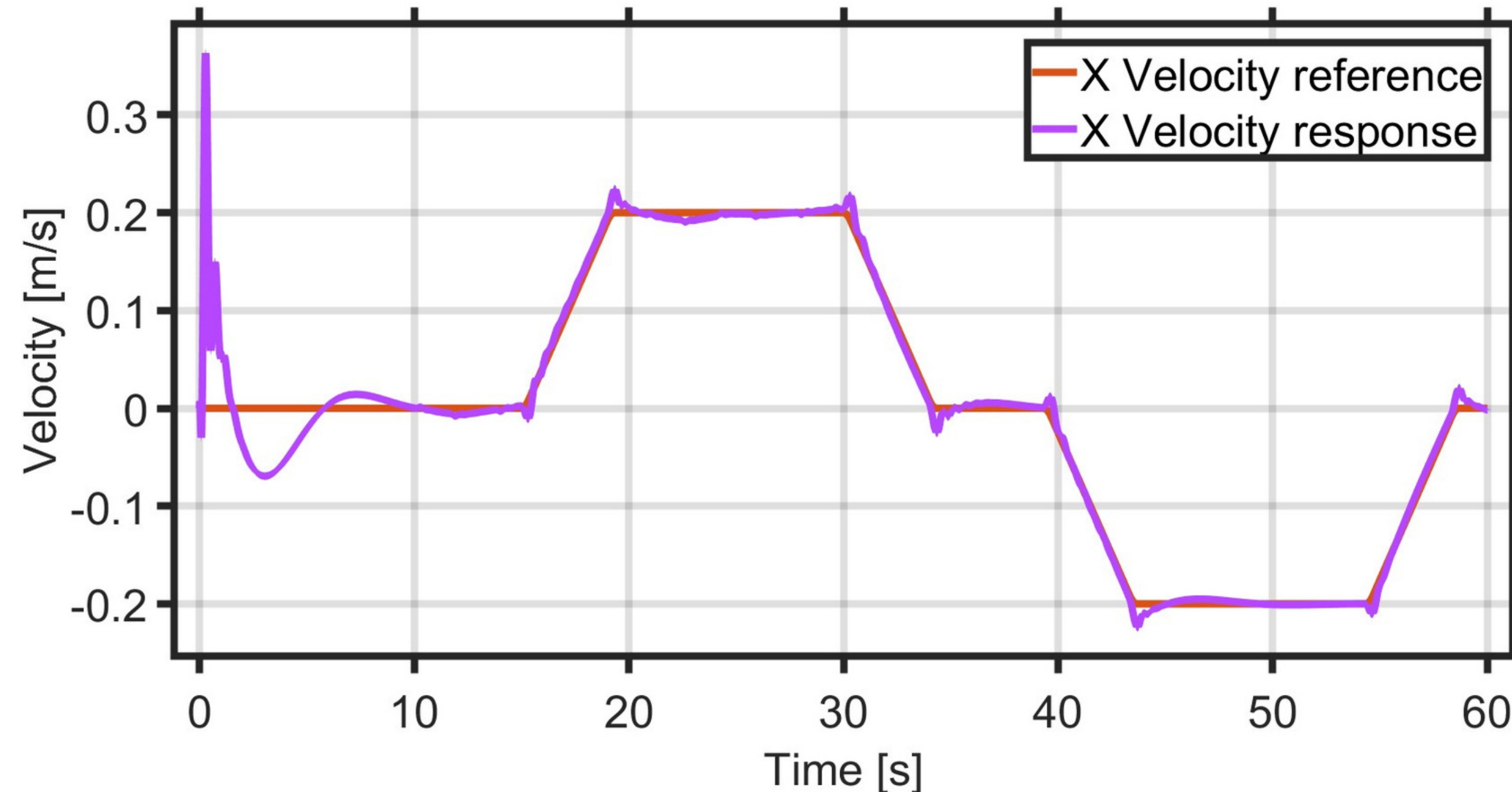
Position error of the robot





# V. Simulation

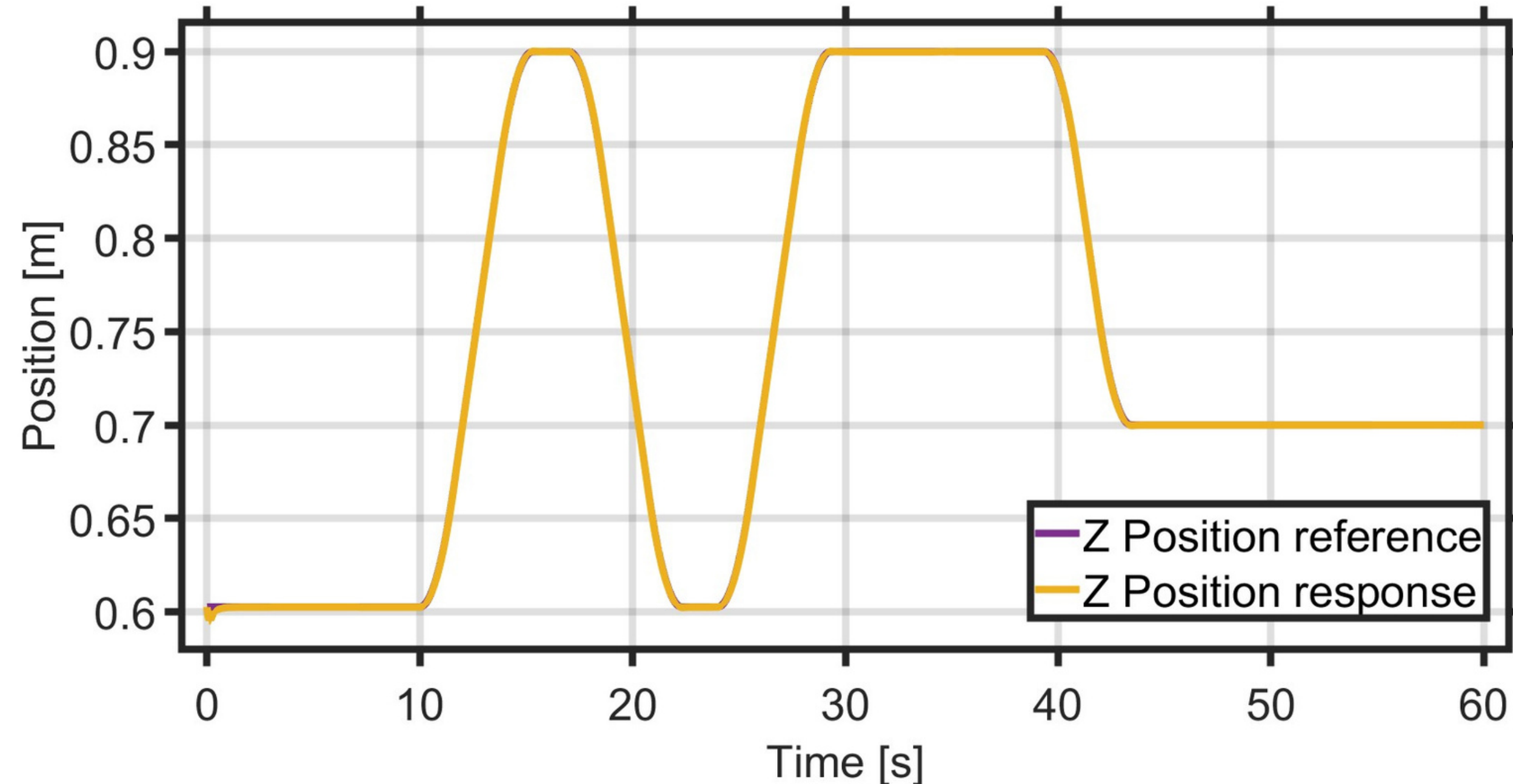
## Horizontal velocity of the robot





# V. Simulation

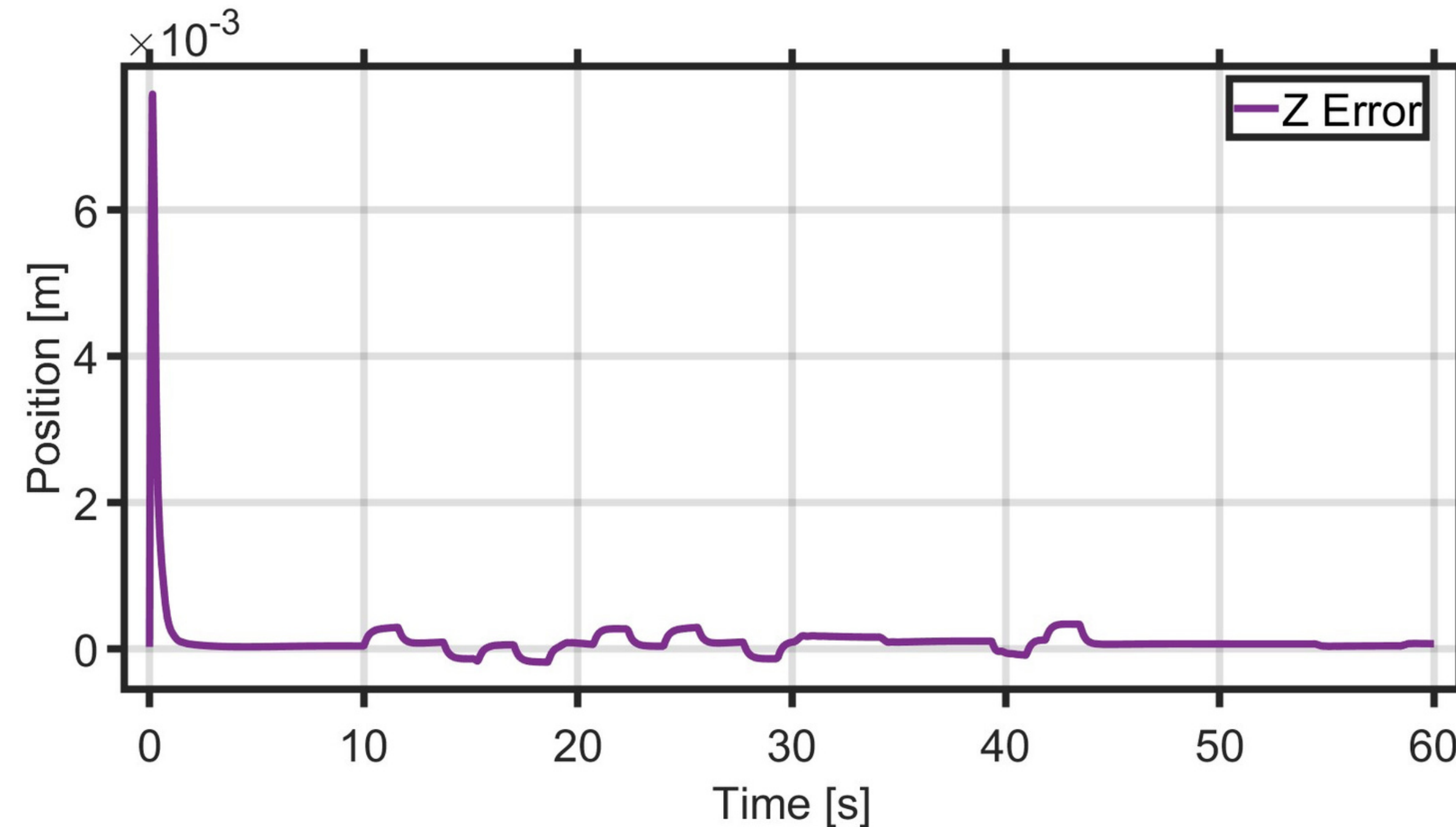
Vertical position of the fork





# V. Simulation

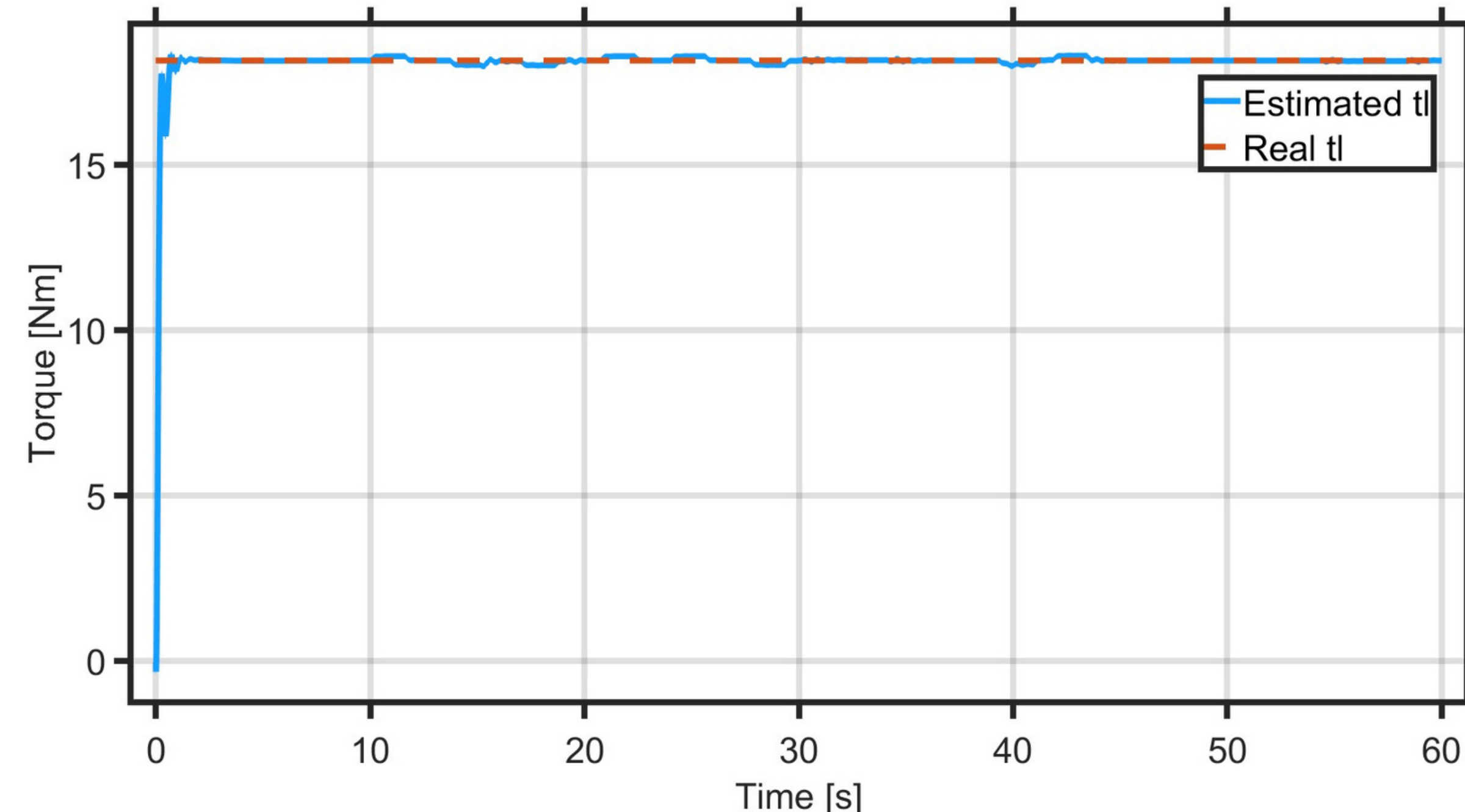
Position error of the fork





## V. Simulation

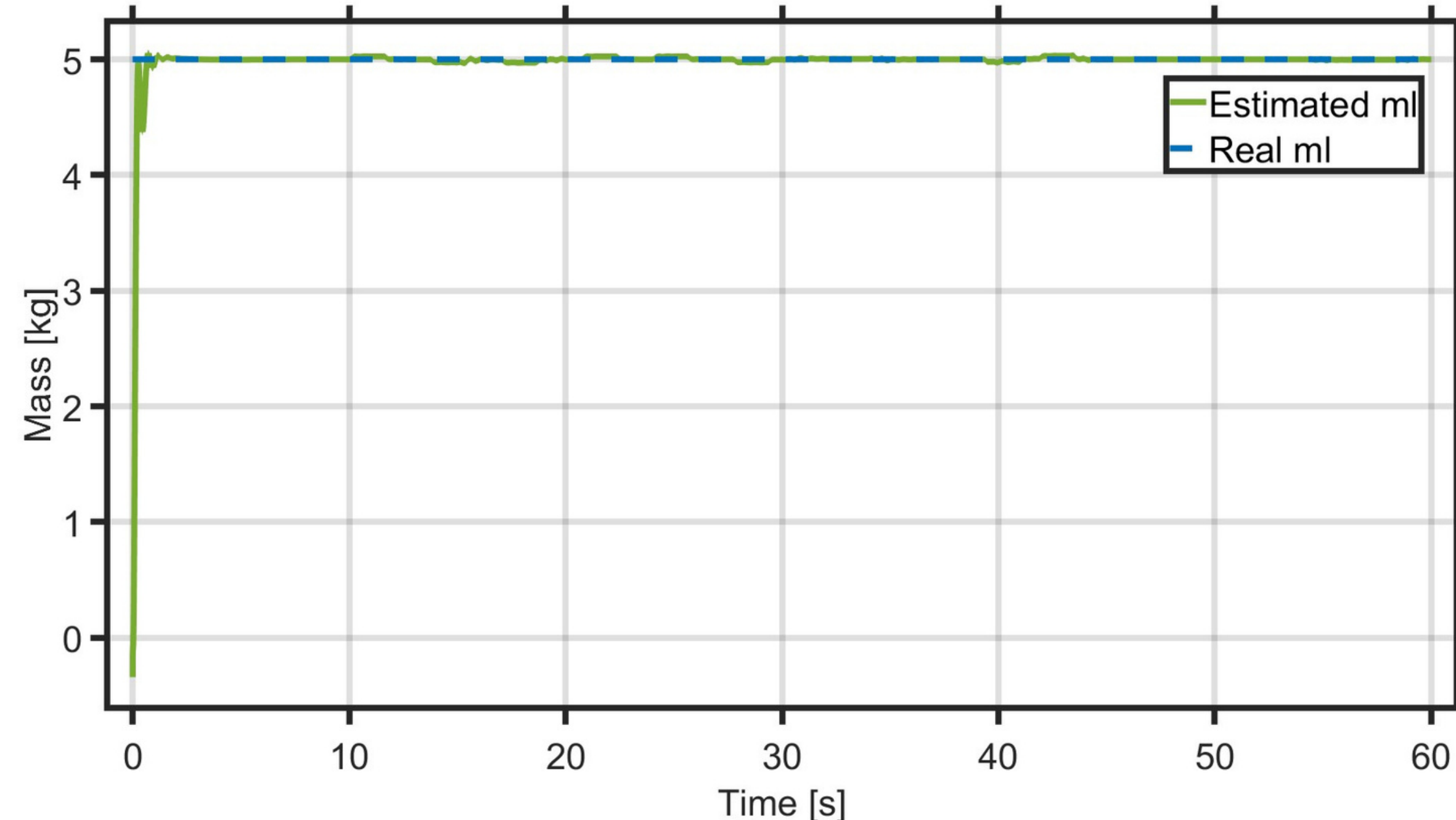
Estimated external torque over the fork (18.142Nm)





## V. Simulation

Estimated mass of the external load (5kg)





# VI. Conclusions and Future work

- The proposed motion planning and control strategies allow the TWFR to execute trajectories in the X and Z coordinate axes simultaneously with an admissible position error.
- The implementation of adaptive IK and ID solutions that depend on the estimation of physical properties of the external load provides great flexibility in industrial environments where it is not possible to control the variables of the load that will be manipulated.
- The next steps for this work are the construction of the lift subsystem and the physical implementation of the presented motion planning and control algorithms.

# References

- [1] P. K. W. Abeygunawardhana, M. Defoort, and T. Murakami, “Self-sustaining control of two-wheel mobile manipulator using sliding mode control”, The 11th IEEE International Workshop on Advanced Motion Control, Mar. 2010. DOI: 10.1109/amc.2010.5464027.
- [2] N. G. K. V. Shihabudheen and G. Dileep, “Applying h-infinity for stability control in two wheeled mobile manipulator”, 2015 International Conference on Soft Computing Techniques and Implementations- (ICSCTI), Oct. 2015. DOI: 10.1109/ICSCTI.2015.7489561.
- [3] J. Ito and T. Murakami, “Underactuated control for two-wheeled mobile robot with an arm using torque constraint conditions and disturbance observer”, 2023 IEEE 32nd International Symposium on Industrial Electronics (ISIE), Jun. 2023. DOI: 10.1109/ISIE51358.2023.10228153.
- [4] H. Kanazawa, K. Ishizaki, Y. Miyata, M. Nawa, N. Kato, and T. Murakami, “Model-based pitch angle compensation for center of gravity variation in underactuated system with an arm”, 2023 IEEE 32nd International Symposium on Industrial Electronics (ISIE), Jun. 2023. DOI: 10.1109/ISIE51358.2023.10228009.
- [5] IEEE, Handle, (accessed Nov.1, 2023): <https://robotsguide.com/robots/handle>.
- [6] F. I. for Material Flow-and-Logistics IML, Evobot - the evolution of autonomous mobile robotic systems, (Accessed Nov.1, 2023): [https://www.iml.fraunhofer.de/en/fields\\_of\\_activity/material-flow-systems/iot-and-embedded-systems/evobot.html](https://www.iml.fraunhofer.de/en/fields_of_activity/material-flow-systems/iot-and-embedded-systems/evobot.html).
- [7] Y. Nagatsu and H. Hashimoto, “Force control for vehicle robot with inverted two wheeled and stable travelling modes”, IECON 2019 - 45th Annual Conference of the IEEE Industrial Electronics Society, 2019. DOI: 10.1109/iecon.2019.8926672.
- [8] A. Gopinath and V. R. Jisha, “Gain scheduled lqr control of a two wheeled mobile robot with heavy payloads”, 2022 IEEE International Conference on Signal Processing, Informatics, Communication and Energy Systems (SPICES), Mar. 2022. DOI: 10.1109/spices52834.2022.9774265.

# References

- [9] V. Klemm and et al., “Ascento: A two-wheeled jumping robot”, 2019 International Conference on Robotics and Automation (ICRA), May 2019. DOI: 10.1109/icra.2019.8793792.
- [10] S. Wang and et al., “Balance control of a novel wheel-legged robot: Design and experiments”, 2021 IEEE International Conference on Robotics and Automation (ICRA), May 2021. DOI: 10.1109/icra48506.2021.9561579.
- [11] E. Ackerman, Tencent’s new wheeled robot flicks its tail to do backflips, (Accessed Nov.1, 2023): <https://spectrum.ieee.org/tencents-new-wheeled-robot-flicks-its-tail-to-do-backflips>.
- [12] F. Raza, W. Zhu, and M. Hayashibe, “Balance stability augmentation for wheel-legged biped robot through arm acceleration control”, IEEE Access, Apr. 2021. DOI:10.1109/access.2021.3071055.
- [13] X. - S. Gao, L. Yan, P. Zhao, N. Du, and S. Bu, “Inverse kinematics solution and analysis for multi-dof mobile manipulator”, 2022 IEEE 17th Conference on Industrial Electronics and Applications (ICIEA), Dec. 2022. DOI: 10.1109/ICIEA54703.2022.10006046.
- [14] S. S. Mathew and V. R. Jisha, “Tracking control of a mobile manipulator with external torque disturbances using computed torque control”, 2020 IEEE 17th India Council International Conference (INDICON), Dec. 2020. DOI: 10.1109/INDICON49873.2020.9342099.
- [15] N. Tan, Z. Zhu, and P. Yu, “Neural-network-based control of wheeled mobile manipulators with unknown kinematic models”, 2020 International Symposium on Autonomous Systems (ISAS), Dec. 2020. DOI: 10.1109/ISAS49493.2020.9378850.
- [16] E. Vollenweider, M. Bjelonic, V. Klemm, N. Rudin, J. Lee, and M. Hutter, “Advanced skills through multiple adversarial motion priors in reinforcement learning”, 2023 IEEE International Conference on Robotics and Automation (ICRA), May 2023. DOI:10.1109/icra48891.2023.10160751.

# References

- [17] C. Schwarke, V. Klemm, M. v. d. Boon, M. Bjelonic, and M. Hutter, “Curiosity-driven learning of joint locomotion and manipulation tasks”, in Proceedings of The 7th Conference on Robot Learning, J. Tan, M. Toussaint, and K. Darvish, Eds., ser. Proceedings of Machine Learning Research, vol. 229, PMLR, Jun. 2023, pp. 2594–2610. [Online]. Available: <https://proceedings.mlr.press/v229/schwarke23a.html>.
- [18] E. Sihite, A. Kalantari, R. Nemovi, A. Ramezani, and M. Gharib, “Multi-modal mobility morphobot (M4) with appendage repurposing for locomotion plasticity enhancement”, *Nature Communications*, vol. 14, no. 1, 2023. DOI: 10.1038/s41467-023-39018-y.
- [19] TOYO Automation Co., Ltd. “ETH2 - 17 Series, in TOYO Electric Actuator Total Catalog Vol. 16, pp. 14–19”. Accessed: 2025-07-02. (2025), [Online]. Available: [https://www.toyorobot.com/File/Fsrv\\_NoAuthority\\_Download/f25011613132034](https://www.toyorobot.com/File/Fsrv_NoAuthority_Download/f25011613132034).
- [A] <https://www.flaticon.com/free-icons/comparison>
- [B] <https://www.flaticon.com/free-icons/standard>
- [C] <https://www.flaticon.com/free-icons/storage>

# Thank you!